GAWBS Noise in Digital Coherent Transmission

Masataka Nakazawa

Tohoku University, 2-1-1 Katahira, Aoba-ku, Sendai, 980-8577, Japan, nakazawa@riec.tohoku.ac.jp

Abstract *Recent research progress on GAWBS noise in single- and multi-core fibers is presented including an analysis of the phase noise spectrum in various optical fibers, the influence of noise on digital coherent transmission, and the noise correlation between cores in four-core fiber. ©2022 The Author(s)*

Introduction

Digital coherent optical transmission with high QAM multiplicity is expected to realize a large transmission capacity with a high spectral efficiency. As the multiplicity increases, the requirements as regards the allowable phase noise become more severe, and therefore, their precise compensation becomes critical. Recently, guided acoustic wave Brillouin scattering (GAWBS) [1-2] has received attention as a new mechanism of signal impairment in digital coherent transmissions [3-13].

This paper presents recent research progress on GAWBS noise in digital coherent transmission. By using three types of single-core fibers (SCFs), it is shown that the GAWBS noise depends strongly on the effective core area A_{eff}. The difference between the GAWBS noise spectra of a multi-core fiber (MCF) and an SCF is also presented in detail including the noise correlation between cores.

GAWBS phase noise in SCF

It is well-known that the GAWBS generated in an SCF has two types of resonance modes, i.e., $R_{0,m}$ modes vibrating only in the radial direction and $TR_{n,m}$ modes vibrating in both the radial and torsional directions. Here, the subscripts n and m represent the order of oscillation in the torsional and radial directions, respectively. The $R_{0,m}$ modes change the refractive index and cause phase noise in the optical signal, while the $TR_{n,m}$ modes change the refractive index along the azimuthal direction and cause not only phase noise but also depolarization due to birefringence. We have evaluated the influence of GAWBS-induced phase noise and depolarization noise on QAM transmission and clarified that the influence of the former is greater than that of the latter [8, 9]. Therefore, we focus on the GAWBS phase noise here.

The GAWBS phase shift $\delta\phi_{n,m}$ is obtained by employing the overlap integral between the refractive index change $\Delta n_{n,m}(r,\theta)$ induced by the $R_{0,m}$ or $TR_{n,m}$ mode and the optical mode field profile $E(r,\theta)$ [1], which is given by

$$\delta\phi_{n,m} = kl\int_0^{2\pi}\int_0^{a}\left\{\Delta n_{n,m}(r,\theta)\times E(r,\theta)\right\} rdrd\theta \,. \quad (1)$$

Here, k is a propagation constant, l is the fiber length, a is the fiber radius, and E is approximated as a Gaussian profile with a mode field diameter $w=\sqrt{A_{\mathrm{eff}}/\pi}$. In ref. [8], we calculated the GAWBS phase noise in three types of SCFs, namely, ULAF, SSMF, and DSF with A_{eff} values of 153, 80, and 45 μm^2, respectively.

Figure 1 shows the mode profile of the optical fields $E(r)$ (blue curve) of ULAF and DSF, and the refractive index change $\Delta n_{0,m}(r)$ (red curve) induced by the $R_{0,5}$, and $R_{0,7}$ modes. These figures show that a high-order $R_{0,m}$ mode provides a better match with the optical field of a smaller A_{eff} fiber.

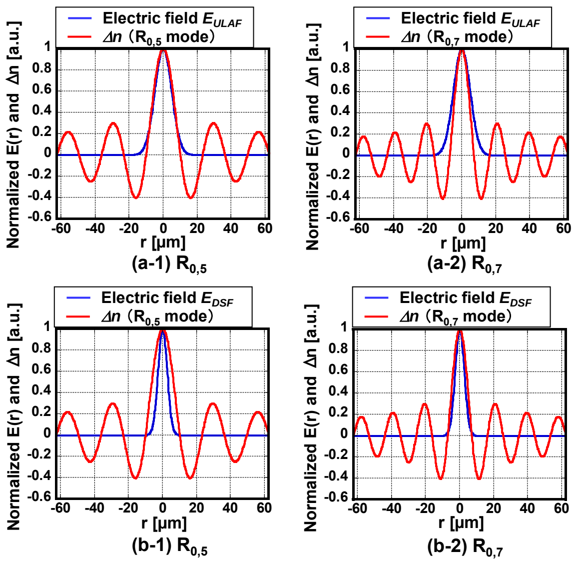

Fig. 1: Comparison of optical field distributions (ULAF and DSF) and refractive index change distributions of $R_{0,5}$, and $R_{0,7}$ modes.

Figure 2 shows the GAWBS phase noise spectra that we measured in 160 km ULAF, 160 km SSMF, and 150 km DSF transmission lines. Here, the calculated results for the $R_{0,m}$ modes are also plotted [8]. The frequency and power of the measured GAWBS noise, which corresponds to each R_{0m} mode, agree well with the calculated results. The ratios of the integrated power of the phase noise components of each fiber were ULAF:SSMF:DSF = 1:1.64:2.30. These results indicate that a smaller A_{eff} results in more efficient GAWBS generation. Therefore, using a large A_{eff} fiber is effective in reducing the GAWBS noise in a digital coherent transmission.

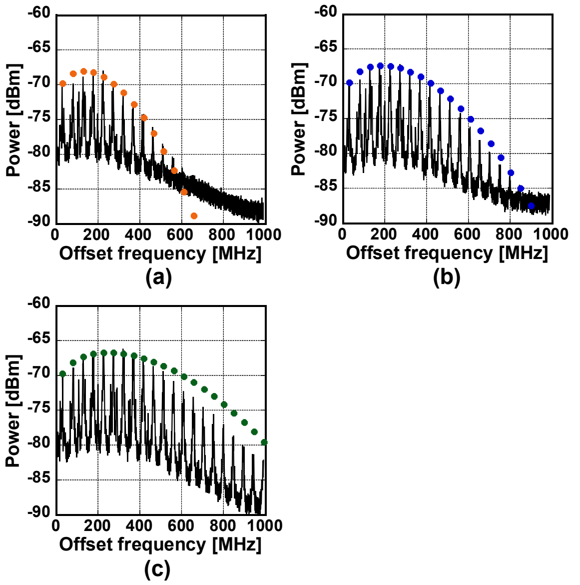

Fig. 2: GAWBS phase noise spectra in SCF. (a) 160 km ULAF, (b) 160 km SSMF, and (c) 150 km DSF. The calculated results for the $R_{0,m}$ modes are also plotted.

GAWBS phase noise in MCF

The GAWBS noise in an MCF with off-center cores has a feature that is quite different from those in SCF since the noise power strongly depends on the optical mode field profile as shown in eq. (1). Figures 3(a)-(e) show the profiles of the refractive index changes caused by the $R_{0,1}$, $TR_{1,2}$, $TR_{2,3}$, $TR_{3,4}$, and $TR_{4,4}$ modes, respectively. The blue and red circles indicate the core positions in SCF and 4CF, respectively.

In SCF, since the mode field is located in the center of the fiber and has a symmetric profile, the overlap integral with $\Delta n_{0,m}$ ($R_{0,m}$ mode) or $\Delta n_{2,m}$ ($TR_{2,m}$ mode), which is symmetric with a peak at the center, has a large value as shown in Fig. 2. The overlap integral between $E(r)$ and $\Delta n_{1,m}$ or $\Delta n_{3,m}$ becomes zero as the TR modes with odd orders have anti-symmetric profiles. In addition, a refractive index change induced by even-ordered TR modes with n ≥ 4 becomes zero at $r = 0$.

In 4CF, in contrast, the mode field is located off-center as shown by the red circles in Fig. 3. This asymmetry reduces the overlap integrals with $\Delta n_{0,m}$ and $\Delta n_{2,m}$. On the other hand, the overlap integral between $E(r)$ and the odd TR modes, such as $\Delta n_{1,m}$ or $\Delta n_{3,m}$, is no longer zero, and the phase shift caused by the odd modes cannot be ignored. In addition, TR modes higher than 4th order also induce a phase shift in MCF.

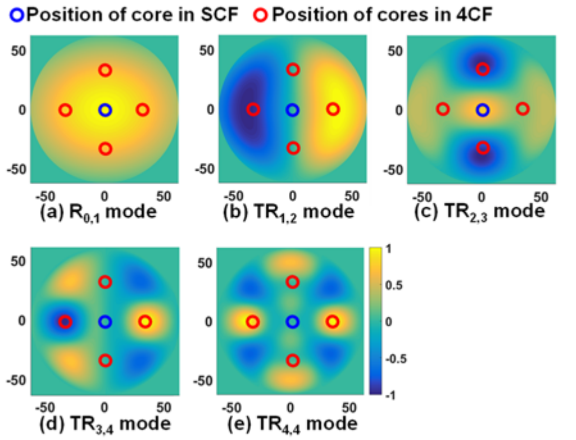

Fig. 3: Refractive-index changes induced by (a) $R_{0,1}$, (b) $TR_{1,2}$, (c) $TR_{2,3}$, (d) $TR_{3,4}$, and (e) $TR_{4,4}$ modes.

Figure 4 shows the GAWBS phase noise spectrum measured in a 36 km 4CF [10], where the calculated results for the $R_{0,m}$ to $TR_{8,m}$ modes are also plotted. It is clearly seen that a larger number of GAWBS components caused by high order $TR_{n,m}$ modes are newly generated in 4CF, resulting in a continuous spectrum. We found that the total phase noise magnitude, which can be obtained by integrating the power spectrum, was almost the same as that in SSMF [10]. This result indicates that the influence of GAWBS in 4CF is comparable to that in SSMF.

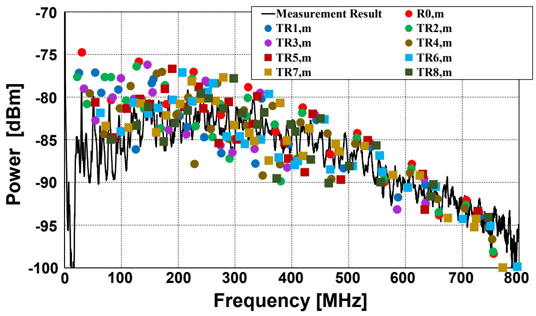

Fig. 4: GAWBS phase noise spectrum in a 36 km 4CF. The calculated results for the $R_{0,m}$ to $TR_{8,m}$ modes are also plotted.

GAWBS limitation in QAM transmission

Here, we describe the influence of the GAWBS phase noise on BER performance in a multi-level coherent QAM transmission with the 4CF. With SCF, we have already shown that the GAWBS phase noise $\delta\Phi_{GAWBS}$ has a Gaussian distribution with the form [8]

$$\delta\Phi_{GAWBS}(z,t)=\sigma_G(z)\times f_r(t). \qquad (2)$$

Here, $f_r(t)$ is a random variable following a Gaussian distribution with a zero mean and a variance of 1, and $\sigma_G(z)$ is the fluctuation of the GAWBS phase noise as a function of the transmission distance. According to ref. [8], $\sigma^2_G(z)$ can be expressed by S x z, where the slope S is 8.8 x 10^{-7} for SSMF. Since the phase noise fluctuation in MCF seems to be similar to that in

SSMF because the noise power level is the same, the noise influence was calculated by using the S value in SSMF. Figure 5 shows the BERs of 64, 256, and 1024 QAM signals impaired by the GAWBS phase noise $\delta\Phi_{GAWBS}$, where the error was counted for a random data sequence with 10^8 symbols in eq. (2). The maximum transmission distance with a BER of 1 x 10^{-2} was limited to 9000, 2600, and 720 km, respectively, for 64, 256, and 1024 QAM transmissions. This result indicates the apparent difficulty of realizing a transoceanic-class QAM transmission with a QAM multiplicity of higher than 64 even without other impairments.

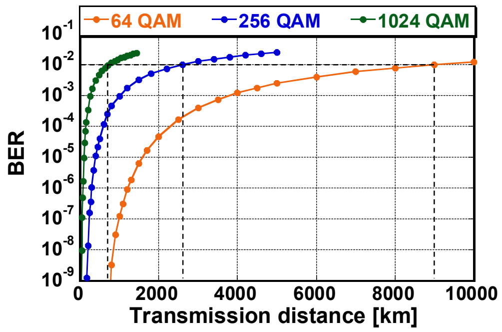

Fig. 5: Numerical analysis of the influence of GAWBS phase noise on BER performance in a multi-level QAM transmission with 4CF.

GAWBS phase noise correlation in MCF

Finally, we describe the GAWBS phase noise correlation between cores in the 4CF [14]. When the correlation is strong, the GAWBS phase noise information, which is detected through one core, may be applied to the phase noise compensation of other cores. For an $R_{0,m}$ mode, such as the $R_{0,1}$ mode as shown in Fig. 3(a), the refractive-index changes of all the cores have the same sign because there are no torsional resonance modes. As a result, there is an in-phase correlation between all the cores. However, the profile of the $TR_{n,m}$ mode has a torsional dependence given by cos(nθ) and sin(nθ) [1, 2]. For an odd-numbered order n, such as the $TR_{1,2}$ and $TR_{3,4}$ modes shown in Figs. 3(b) and 3(d), respectively, there is no correlation between adjacent cores, while there is an out-of-phase correlation between crossed cores because the signs of the refractive index change are opposite. For an even-numbered order n except for a multiple of 4, such as the $TR_{2,3}$ mode shown in Fig. 3(c), there is an out-of-phase correlation between adjacent cores, but there is an in-phase correlation between crossed cores. When n is a multiple of 4, such as the $TR_{4,4}$ mode shown in Fig. 3(e), there is an in-phase correlation between all the cores. As a result, 4CF has various degrees of correlation depending on the order n.

We calculated the GAWBS phase noise for each core by using eq. (1) and evaluated the correlation C between them by using the following equation.

$$C = \delta\phi_i \cdot \delta\phi_j \Big/ \sqrt{\left|\delta\phi_i\right|^2 \left|\delta\phi_j\right|^2}\ . \qquad (3)$$

Here, $\delta\phi_i$ and $\delta\phi_j$ are GAWBS phase noises in cores #*i* and #*j*, respectively. Figure 6(a) shows the calculated correlation coefficients between adjacent cores, where the order n dependence of the correlation can be clearly seen. The measured GAWBS phase noise correlation between adjacent cores is shown in Fig. 6(b). We employed heterodyne detection to evaluate the correlation of the GAWBS phase noise generated in different cores [14]. The black horizontal line shows the -3 dB level, which corresponds to the power level obtained when uncorrelated noises are added incoherently in the heterodyne detection. The regions higher and lower than this black horizontal line correspond to the in-phase and out-of-phase correlations, respectively. We see that the calculated and measured results are in good agreement. The same results are obtained for the correlation between crossed cores [14]. These results indicate that the correlation between cores strongly depends on the order n and the core position. Namely, the GAWBS phase noise induced in one core differs greatly from that induced in another core. Therefore, it is necessary to detect the GAWBS phase noise with a pilot tone in each core independently when employing a reverse phase modulation technique for GAWBS phase noise compensation [3]

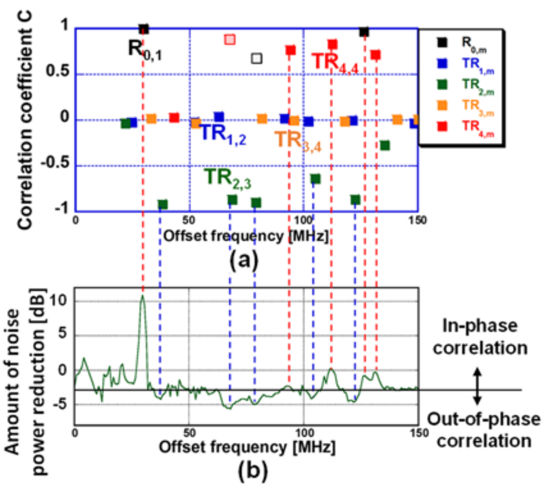

Fig. 6: GAWBS phase noise correlation between adjacent cores in 4CF. (a) Calculated and (b) measured results.

Conclusions

We presented recent research progress on the GAWBS noise in SCF and MCF. GAWBS noise compensation will play an important role in transoceanic-class digital coherent transmission when the signal multiplicity exceeds 64 QAM.

References

[1] R. M. Shelby, M. D. Levenson, and P. W. Bayer, "Resolved forward Brillouin scattering in optical fiber," Phys. Rev. Lett., vol. 54, no. 9, pp. 939-942 (1985).

[2] R. M. Shelby, M. D. Levenson, and P. W. Bayer, "Guided acoustic-wave Brillouin scattering," Phys. Rev. B, vol. 31, no. 8, pp. 5244-5252 (1985).

[3] M. Nakazawa, M. Yoshida, M. Terayama, S. Okamoto, K. Kasai, and T. Hirooka, "Observation of guided acoustic-wave Brillouin scattering noise and its compensation in digital coherent optical fiber transmission," Opt. Express, vol. 26, no. 8, pp. 9465-9181 (2018).

[4] M. Nakazawa, M. Terayama, S. Okamoto, M. Yoshida, K. Kasai, and T. Hirooka, "Observation of guided acoustic-wave Brillouin scattering and its digital compensation in coherent QAM transmission," in Proc. OFC2018, paper M4B.2.

[5] M. A. Bolshtyansky, J. -X. Cai, C. R. Davidson, M. V. Mazurczyk, D. Wang, M. Paskov, O. V. Sinkin, D. G. Foursa, and A. N. Pilipetskii, "Impact of spontaneous guided acoustic-wave Brillouin scattering on long-haul transmission," in Proc. OFC2018, paper M4B.3.

[6] M. Paskov, M. A. Bolshtyansky, J. -X. Cai, C. R. Davidson, D. G. Foursa, and A. N. Pilipetskii, "Observation and compensation of guided acoustic-wave Brillouin scattering in modulated channels," Proc. OFC2019, paper Tu3J.3.

[7] M. Yoshida, N. Takefushi, K. Kasai, T. Hirooka, and M. Nakazawa "Suppression of large error floor in 1024 QAM digital coherent transmission by compensating for GAWBS phase noise," Opt. Express, vol. 27, no. 25, pp. 36691-36698 (2019).

[8] N. Takefushi, M. Yoshida, K. Kasai, T. Hirooka, and M. Nakazawa "Theoretical and experimental analyses of GAWBS phase noise in various optical fibers for digital coherent transmission," Opt. Express, vol. 28, no. 3, pp. 2873-2883 (2020).

[9] M. Yoshida, N. Takefushi, K. Kasai, T. Hirooka, and M. Nakazawa, "Precise measurements and their analysis of GAWBS-induced depolarization noise in various optical fibers for digital coherent transmission," Opt. Express, vol. 28, no. 23, pp. 34422–34433 (2020).

[10] N. Takefushi, M. Yoshida, K. Kasai, T. Hirooka, and M. Nakazawa, "GAWBS phase noise characteristics in multi-core fibers for digital coherent transmission," Opt. Express, vol. 28, no. 15, pp. 23012-23022 (2020).

[11] V. Ivanov, J. Downie, and S. Makovejs, "Modeling of guided acoustic waveguide Brillouin scattering impact in long-haul fiber optic transmission systems," in Proc. ECOC2020, paper Tu2E-6.

[12] F. Yaman, K. Nakamura, E. Mateo, S. Fujisawa, H. G. Batshon, T. Inoue, Y. Inada, and T. Wang, "Guided acoustic Brillouin scattering measurements in optical communication fibers," Optics Express Vol. 29, no. 11, pp. 17628-17668 (2021).

[13] M. Yoshida, K. Sato, T. Hirooka, K. Kasai, and M. Nakazawa, "Precise measurements and their analysis of GAWBS-induced depolarization noise in multi-core fiber for digital coherent transmission," IEICE Trans. Comm., vol. E105-B, no. 2, pp. 151-158 (2022).

[14] K. Sato, M. Yoshida, K. Kasai, T. Hirooka, and M. Nakazawa, "GAWBS noise correlation between cores in multi-core fibers," Opt. Express, vol. 29, no. 26, pp. 42523-42537 (2021).